

Ab initio analysis of magnetovolume versus chemical effects in

CeRuSi and its hydride

Samir F. Matar

Institut de Chimie de la Matière Condensée de Bordeaux (ICMCB) - CNRS.

Université Bordeaux 1. 33608 Pessac Cedex, France.

(Dated: March 29, 2007)

Abstract

The change from heavy Fermion to antiferromagnetic behavior of intermetallic system CeRuSi upon hydrogenation is addressed on bases of lattice expansion and chemical bonding effects within the density functional theoretical framework using all electrons scalar relativistic augmented spherical wave ASW method. While no magnetic moment develops in the 111 system, from total energy differences, the hydride is found to be stable as an antiferromagnet in the ground state in agreement with experiment. The role of anisotropic lattice expansion induced by hydrogen insertion is shown to be prevailing over the chemical bonding between hydrogen and the metallic species especially cerium.

PACS numbers: 07.55.Jg, 71.20.-b, 71.23

I. INTRODUCTION AND CONTEXT

Intermetallic systems based on cerium $Ce_xT_yX_z$ (T = transition metal and X = p-metal) are known to exhibit a wide variety of electronic properties such as heavy Fermions, valence fluctuation, magnetic ordering, ... [1–3]. The underlying physics of these properties is relevant to the degree of hybridization between the (f) states and the conduction electrons (c). The interaction at each lattice site, between conduction electrons and localized 4f electrons is described by the Kondo model whereby conduction electrons are spin polarized due to their exchange interaction with the localized 4f electrons. This spin polarization propagates from one lattice site to another. Being the first element in the rare earth series, cerium is considered as a border case where the degree of delocalization of 4f states depends on the applied pressure as well as on the crystal environment. In electronic structure calculations this delicate situation is addressed through various approaches treating the 4f states either as atomic like core states or as itinerant in the framework of the local spin density approximation LSDA [4] to the density functional theory DFT [5]. This duality was experimentally evidenced in a combined analysis of μ SR (muon spin relaxation) and neutron experiments on cerium intermetallic systems which reveals the existence of magnetic excitations due to both conduction electrons at the Fermi level and well localized f-electrons [6]. Regarding the lattice environment, the quantum mixing (hybridization) of the 4f states with those of the ligand states can have large effects as well. This involves chemical bonding properties, which are dependent of the crystal lattice properties (structure and interatomic distances). For rare earth elements belonging to the middle of the series the degree of localization of f states becomes important and the treatment of itinerant as well as localized electrons within the same theoretical framework imposes the use of self interaction corrections (SIC) [7] which cancel the erroneous effects of the interaction of an electron with itself as obtained by the LSDA. That was recently applied to the electronic structures of europium chalcogenides and pnictides [8]. Generally compounds based on cerium are magnetically ordered at normal pressure and become non magnetic at high pressures. Insertion of light elements such as hydrogen can mimic negative pressures with drastic consequences on the magnetic properties of Ce based intermetallics. Two effects can occur: On one hand, the expansion of the lattice by hydrogen intake should lead to an enhancement of the localization of the 4f states due to less quantum mixing between them such as in the intermediate valence

CeNiIn which transforms into a long-range magnetically ordered ferromagnet with trivalent Ce in the hydride [9] but on the other hand the chemical bonding between the valence states of Ru, Si and especially Ce with H ligand could induce a decrease of the magnetization whence a decrease of the local magnetic moment and, eventually, a loss of magnetization such as in CeCoSiH [10] and CeCoGeH [11]. Recently Chevalier [12] evidenced that CeRuSi forms a stable hydride CeRuSiH_{1.0} when it is exposed to hydrogen at moderate conditions of pressure and temperature. A transition from a heavy Fermion state to a magnetically ordered state with antiferromagnetic behavior upon hydrogen insertion was identified. In present communication we focus on the theoretical approach within the DFT of the interplay between lattice expansion and chemical bonding effects to the electronic and magnetic structures within CeRuSi and its hydride.

II. ELECTRONIC STRUCTURE CALCULATIONS

A. Crystal structure

The investigation of the structural properties of CeRuSi and of its hydride CeRuSiH_{1.0} using X-ray powder diffraction [12] indicates that they both crystallize in the tetragonal CeCoGeH-type structure (space group $P4/nmm$ N^o 129) [11]. This structure shown in fig. 1 can be described by a stacking along the c -axis of two layers formed by [Ce₄Ru₄] antiprisms and separated by one layer of [Ce₄] pseudo-tetrahedral units. The insertion of H-atoms within the [Ce₄] pseudo-tetrahedral sites gives an interatomic distance $d_{Ce-H} = 2.444 \text{ \AA}$ between Ce and H atoms which is somehow larger than its magnitude within the isostructural CeCoSiH system [13] so that less bonding is expected between the two atomic species. We can also note that the hydrogenation of the ternary silicide causes a pronounced anisotropic expansion of the unit cell; the a -parameter increases with 0.4 % whereas the c -parameter increases strongly from 6.894 \AA to 7.514 \AA ($\sim 9 \%$). In other words, the insertion of hydrogen into CeRuSi involves an expansion of the unit cell volume from 121.43 \AA^3 to 131.24 \AA^3 . The $\sim 8.1 \%$ volume expansion is slightly larger than within CeCoSi ($\sim 7.8 \%$) which equally undergoes an anisotropic lattice expansion [13].

B. Methodology

For the band structure calculations we used the augmented spherical wave (ASW) method in its scalar-relativistic implementation [14, 15] with Vosko, Wilk and Nusair implementation for the LSDA scheme [16]. In the ASW method, the wave function is expanded in atom-centered augmented spherical waves, which are Hankel functions and numerical solutions of Schrödinger's equation, respectively, outside and inside the so-called augmentation spheres. The choice of the augmentation radii were automatically determined using the sphere-geometry optimization algorithm [17]. The Brillouin zone integrations were performed using the linear tetrahedron method with up to 126 \mathbf{k} -points within the irreducible wedge. Here we use a new version of the ASW code, which takes the non-spherical contributions to the charge density inside the atomic spheres into account. All valence electrons, including 4f (Ce) were treated as band states. In the minimal ASW basis set, we chose the outermost shells to represent the valence states and the matrix elements were constructed using partial waves up to $l_{max}+1 = 4$ for Ce, $l_{max}+1 = 3$ for Ru, $l_{max}+1 = 2$ for Si and $l_{max}+1 = 1$ for H. The completeness of the valence basis set -without calling for semi core states- was checked at all volumes for charge convergence with $l_{max}+1$ occupation less than 0.1 electron. Regarding the angular momentum expansions, they are in principle carried to infinity. For details on the ASW method the reader is referred to recent comprehensive work [18]. The self-consistent field calculations are run to a convergence of $\Delta Q=10^{-8}$ Ryd and the the accuracy of the method is in the range of about 0.1 to 1 meV regarding energy differences.

In a first step the calculations were carried out assuming non-magnetic configurations (non spin polarized NSP), meaning that spin degeneracy was enforced for all species. Such a configuration is not relevant to a paramagnet which could be simulated by a huge supercell entering random spin orientations over the different magnetic sites. However disordered local moment approach based on coherent potential CPA approximation [19] or LDA+DMFT approach [20] can be used for this purpose.

Then spin polarized calculations leading to an implicit long range ferromagnetic order were carried out; spin orbit coupling effects were accounted for as well within subsequent fully relativistic calculations using the Dirac equation [21]. In order to provide a model for the experimentally observed antiferromagnetic ground state of the hydride system we have

constructed a double unit cell along the c -axis. In view of non available neutron diffraction characterizations this provides one possible model of a long range AF spin structure which should be validated as a ground state configuration from the relative energies of the band theoretical calculations.

To extract more information about the nature of the interactions between the atomic constituents from electronic structure calculations, the crystal orbital overlap population (COOP) [22] or the crystal orbital Hamiltonian population (COHP) [23] may be employed. Both approaches provide a qualitative description of the bonding, nonbonding and antibonding interactions between two atoms although COOP description, when defined within plane-wave basis sets, exaggerates the magnitude of antibonding states. A slight refinement was recently proposed in form of the "energy of covalent bond" (ECOV), which combines COHP and COOP to calculate quantities independent of the choice of the zero of potential [24]. In the present work the ECOV criterion was used for the chemical bonding analysis. In the plots, negative, positive and zero ECOV magnitudes are relevant to bonding, antibonding and nonbonding interactions respectively.

C. Non spin polarized configuration

NSP calculations provide a description of the system as a function of energy positions of the site projected density of states DOS as well as an assessment of the chemical bonding. This is related to the fact that the spin polarized bands, to a large degree, result from the NSP bands by a rigid energy shift. Hence it is well justified to discuss the chemical bonding already from the NSP results. At self consistency little charge transfer could be observed between atomic species thus pointing to the covalent (metallic character) of the studied systems. The site projected DOS provide a better description of the quantum mixing between valence states. This is provided for CeRuSi and CeRuSiH_{1.0} in fig. 2 a and b. In both panels the Fermi level (E_F) is taken as zero energy. The cerium DOS are seen to prevail through the large peak around E_F mainly due to (4f) Ce states which show larger localization (sharper and narrower peaks) in the hydride system despite similar magnitude of DOS at the Fermi level of $\sim 3 \text{ eV}^{-1}$ for both systems. This is concomitant with a larger cell volume whereby the average Ce-Ce separation is higher. But there is a non negligible contribution from Ce itinerant states below E_F which ensure for the chemical

bonding through the hybridization with Ru and Si states as well as with hydrogen as it will be shown below. Due to the large filling of their d-states, Ru DOS are found completely within the valence band. They show similar shape at the low energy part of the valence band (VB), which is a feature pointing to a mixing between Ru, Si and Ce. Silicium states contribute to the bonding essentially with ruthenium. Within the hydride system hydrogen partial DOS (PDOS) were artificially multiplied by 10 in order to clearly exhibit their contribution within the VB where Ce states are prevailing. They can be seen to have a similar skyline to other states between -6 and -4 eV with significant mixing with Ce itinerant states.

This is stressed by the band structure plotted along the main lines of the simple tetragonal Brillouin zone in 3 (a, b). From fig. 3 a, there is a large dispersion of the bands at the bottom of the VB signaling s, p like states due to hydrogen as well as Si while localized states around the Fermi level are due to Ce 4f states; in between, i.e. in the energy range -4, 0 eV the transition metal bands are present. The H contribution is shown in fig.3 b by the fat bands (full lines are stressed by dotted lines) which are found mainly with a large dispersion at the bottom of the VB as suggested above, whence the preserved s character of hydrogen, and around the Fermi level where Ce bands are found which points to their mixing. However there is a better account of the hybridization features from chemical bonding criteria.

Two-body interactions between atomic species are described by covalent bond energy ECOV criterion in fig. 4 a-c. Negative, positive and zero values along the y-axis are relative to bonding, antibonding and non-bonding states respectively. Because of their little involvement with the bonding (4f) Ce orbitals were discarded from the analysis. In fig. 4 a and b we make explicit the ECOV for Ce-Ru, Ce-Si and Ru-Si pair interactions which determine the nature of the bonding within the pristine and hydrided ternary systems respectively. The major part of the VB is bonding with antibonding interactions starting to appear in the neighborhood of E_F especially for Ru-Si. The difference appears as well for the Ce-Ru and Ru-Si bonding which show larger overall magnitudes in $\text{CeRuSiH}_{1.0}$ than in CeRuSi . This is opposite to the formerly studied isostructural CeCoSi and its hydride [10]. While the shorter Ru-Si spacing between Ru and Si within the hydride (2.36 Å versus 2.41 Å in pristine CeRuSi) could explain the enforced Ru-Si bonding, the distance criterion for the Ce-Ru does not stand for explaining the enforcement of the Ce-Ru bond within the hydride. The strengthening of the Ce-Ru bonding within the hydride is probably in line with the larger itinerant population of Ce within CeRuSiH as observed from the calculations through

the increase of both 5d and 4f occupations and which is equally exhibited by the stronger localization of the Ce(4f) DOS within the hydride (fig. 2b). Turning to the bonding with hydrogen, fig. 4 c gives the different contributions. Here the prevailing interaction is for Ce-H which follows from the shortest distance within the lattice: $d_{Ce-H} = 2.444 \text{ \AA}$; while $d_{Si-H} = 3.359 \text{ \AA}$ and $d_{Ru-H} = 3.756 \text{ \AA}$, on one hand and from the tetrahedral Ce environment of H on the other hand. Ce-H interaction is bonding throughout the VB and above E_F . On the contrary there are antibonding contributions for Ru-H around -2 eV and Si-H bonding is expectdely negligible from distance criteria.

D. Spin polarized configurations

Beside calculations of CeRuSi and CeRuSiH_{1.0} at experimental volumes, additional calculations were done for the equiatomic alloy system at the hydride volume and vice versa in order to assess the volume versus chemical effects due to H insertion.

1. Energies and magnetovolume effects

Calculations for the magnetic structures were carried out by initially allowing for two spin occupations, then self-consistently converge the charges and the magnetic moments. Firstly we assumed a ferromagnetic SP- F configuration with no constraint on spins. For CeRuSiH_{1.0} further antiferromagnetic AF computations were carried out for checking whether the experimentally evidenced AF ground state would actually be found from energy differences with respect to the SP- F hypothesis.

Self consistent SP calculations of the alloy system CeRuSi provide zero magnetization with no spin polarization of any of the valence bands; this coincides with the heavy Fermion behavior but should be considered as fortuitous in the framework of the LSDA approximation. The energy difference between the NSP and SP configuration is nil because there is no gain of energy due to exchange. Expanding the alloy lattice to the hydride volume in a progressive way did not lead to the development of magnetization upon successive self consistent computations, i.e. up to 7.5% volume increase. At a volume increase of $\sim 8\%$ i.e., at the hydride volume, there is an onset of magnetization such that $M(\text{Ce})=0.34 \mu_B$, $M(\text{Ru})= -0.013 \mu_B$ which is of induced nature due to Ce moment and vanishingly small Si

moment. This underlines the magnetovolume effects induced by hydrogen. For the hydride system, the SP- F configuration provides an energy stabilization of $\Delta E = -3.264$ meV and the development of ordered atomic magnetic moments such that: $M(\text{Ce})=0.58 \mu_B$, $M(\text{Ru})=0.004 \mu_B$, $M(\text{Si})=0.0036 \mu_B$ and $M(\text{H})= -0.0013 \mu_B$. The negative value of the induced moment on H arises from the quantum mixing of its valence states with nearest neighboring Ce. The different magnitudes of Ce moments at the same volume between the two calculations with an enhanced $M(\text{Ce})$ in the hydride, point both to the anisotropic effect of the lattice expansion and to the fact that H does not reduce the magnitude of the magnetization due to the chemical bonding effects (cf. fig. 4-c).

Further calculations including spin orbit coupling effects were carried out. This is because the localized character of the 4f wave function leads to the formation of orbital moments. We used the orbital field (OR) scheme introduced by Brooks [1] and Sandratskii and Kübler [25] which helped to account for the experimental moments within formerly studied Ce intermetallic systems [3]. The trend is that the magnitude of the orbital moment (L) is close to that of the spin-only (S.O.) moment but with opposite signs in agreement with Hund's 3rd rule. The L moment of cerium stems from a 4f (Ce) occupation of about 1.3 electrons whose orbital moment ($\sim 2.5 \mu_B$) comes close to the one of an atomic orbital, namely $3 \mu_B$ as expected from Hund's 2nd rule. This reflects the atomic like character of the 4f (Ce) shell. A resulting ordered LS moment of cerium of $\sim 1.78 \mu_B$ was found for the ferromagnetic configuration while a larger magnitude ($\sim 1.9 \mu_B$) arising from the smaller spin only moment within the AF configuration is obtained. The computed values should be confronted with experimental magnetizations from neutron diffraction when they are made available. In order to complete the discussion on the magnetovolume effects, we have also calculated CeRuSiH_{1.0} with and without H at the 111-alloy volume. The resulting moments are respectively $M(\text{Ce})=0.22 \mu_B$ and $M(\text{Ce})= 0.37 \mu_B$. The global decrease as with respect to the actual hydride system is mainly due to the reduced volume. But one can also suggest when H is present that the smaller Ce-H distance should induce large chemical bonding effects between Ce and H whereby the Ce moment is decreased furthermore.

2. Antiferromagnetic configuration

First antiferromagnetic AF computations within one cell of CeRuSiH_{1.0} with one formula unit polarized as up-spin (\uparrow) the other as down-spin (\downarrow) could not lead to a stable configuration, i.e. atomic magnetic moments vanished. This led to build the AF cell by doubling tetragonal CeRuSiH_{1.0} along the c-axis. The whole unit cell was then set to develop spin \uparrow atoms for one subcell and spin \downarrow atoms for the other subcell, i.e. with a magnetic vector $q : [0, 0, \frac{1}{2}] \frac{2\pi}{c}$ along Oz. At self consistency $\Delta E = -1.3$ meV in favor of antiferromagnetic ordering was obtained thus pointing to SP-*AF* ground state in agreement with experiment. The total magnetization is zero with $M_{subcell} = \pm 1.153 \mu_B$ and $M(\text{Ce}) = \pm 0.56 \mu_B$, i.e., slightly smaller than in the SP-*F* configuration which is likely due to the decrease of symmetry.

3. Analysis of the density of states

The effects of spin polarization for the CeRuSiH_{1.0} are illustrated for the site and spin projected DOS given in fig. 5. In as far as these effects are not present for CeRuSi its SP DOS are not shown. The site projected DOS show an energy shift between the electron populations for the majority (\uparrow) and minority (\downarrow) spin populations mainly for Ce which carries a magnetic moment. The induced nature of Co moment in formerly studied CeCoSi [10] is no more observed here and Ru which carries a vanishingly small moment can be seen to have nearly equal DOS weights between (\uparrow) and (\downarrow) PDOS. This is likely due to the nature of d states involved, i.e. 3d versus 4d states, whereby Co(3d) are closer to the Fermi level and hence mix further with the Ce states carrying the magnetic moment. Hydrogen PDOS, artificially multiplied by 10, are shown to have larger contribution in the lower part of the VB as expected from the available valence states. However due to the relatively strong Ce-H bond (cf. fig. 3c) small intensity PDOS can be observed around the Fermi level, i.e. around Ce(4f) states, whence the induced character of the H moment.

III. CONCLUSION

In this work we have undertaken a theoretical analysis of the hydrogen insertion effects on the magnetic behavior of CeRuSi equatomic system. Contrary to formerly studied CeCoSi

and its hydride (transformation from AF \rightarrow spin fluctuating system), the heavy Fermion behavior of CeRuSi changes to an antiferromagnet upon hydrogen absorption. In order to further address this peculiar feature we have undertaken *ab initio* computations within the local spin density functional theory for CeRuSi for the hydride CeRuSiH at experimental volumes. Analyses of the electronic structures and of the chemical bonding properties using the covalent bond energy lead to suggest that the chemical effect of hydrogen does not prevail over cell expansion which enhances the magnetization. A possible antiferromagnetic structure with a propagation along the c axis was proposed for CeRuSiH ground state which is experimentally evidenced in this work from magnetic measurements.

IV. ACKNOWLEDGEMENTS

Discussions with Dr Volker Eyert of the University of Augsburg - Germany, are gratefully acknowledged. I wish to thank Dr Bernard Chevalier of the ICMCB-CNRS for providing the crystal data prior to publication. Computations were carried out on main frame computers of the M3PEC-Mésocentre, University Bordeaux 1 (<http://www.m3pec.u-bordeaux1.fr>), financed by the “Conseil Régional d’Aquitaine” and the French Ministry of Research and Tecnology.

-
- [1] M.S.S. Brooks, B. Johansson, in: K. H. J. Buschow (Ed.), Handbook of Magnetic Materials, Vol. **7** (1993).
 - [2] G. R. Stewart. Rev. Modern Phys., **73** 797 (2001).
 - [3] S.F. Matar and A. Mavromaras. J. Solid State Chemistry, **149** 449 (2000).
 - [4] D. M. Ceperley and B. J. Alder. Phys. Rev. Lett., **45** 1196 (1980).
 - [5] W. Kohn and L. J. Sham, Phys. Rev. A, **140** 1133 (1965); P. Hohenberg and W. Kohn, Phys. Rev. B **136** 864 (1964).
 - [6] A. Yaouanc, P. Dalmas de Rotier, P. C. M. Gubbens, C. T. Kaiser, P. Bonville, J. A. Hodges, A. Amato, A. Schenck, P. Lejay, A. A. Menovsky and M. Mihalik. Physica B: Condens. Matter. **259-261** 126 (1999).1
 - [7] J.P. Perdew and Alex Zunger. Phys. Rev. B **23** 5048 (1981).

- [8] M. Horne, P. Strange, W. M. Temmerman, Z. Szotek, A. Svane and H. Winter. *J. Phys.: Condens. Matter* **16** 5061 (2004).
- [9] S.F. Matar, B. Chevalier, V. Eyert, J. Etourneau. *Solid State Sciences* **5** 1385 (2003).
- [10] B. Chevalier and S.F. Matar. *Phys. Rev. B* **70** 174408 (2004).
- [11] B. Chevalier, S.F. Matar, M. Ménetrier, J. Sanchez Marcos and J. Rodriguez Fernandez. *J. Phys. Cond. Matter* **18** 6045 (2006).
- [12] B. Chevalier, Internal CNRS report. Private communication (2006).
- [13] B. Chevalier, J. Etourneau, J. Rossat-Mignod, R. Calemczuk and E. Bonjour. *J. Phys.: Condens. Matter.* **3** 1847 (1991).
- [14] A. R. Williams, J. Kübler, and C. D. Gelatt, Jr., *Phys. Rev. B* **19**, 6094 (1979).
- [15] V. Eyert, *Int. J. Quantum Chem.* **77**, 1007 (2000).
- [16] S. H. Vosko, L. Wilk, and M. Nusair, *Can. J. Phys.* **58**, 1200 (1980)
- [17] V. Eyert and K.-H. Höck, *Phys. Rev. B* **57**, 12727 (1998).
- [18] V. Eyert, *The Augmented Spherical Wave Method – A Comprehensive Treatment, Lecture Notes in Physics* (Springer, Heidelberg, 2007).
- [19] A. M. N. Niklasson, J. M. Wills, M. I. Katsnelson, I. A. Abrikosov, O. Eriksson, B. Johansson. *Phys. Rev. B* **67** 235105.1-235105.6 (2003).
- [20] I. A. Nekrasov, K. Held, N. Blümer, A. I. Poteryaev, V. I. Anisimov, D. Vollhardt. *Eur. Phys. J., B Cond. Matter Phys.* **18** 55 (2000).
- [21] J. Sticht. Ph. D. Thesis, D17, University of Darmstadt, Germany (1989).
- [22] R. Hoffmann, *Angew. Chem. Int. Ed. Engl.* **26** 846 (1987).
- [23] R. Dronskowski and P. E. Blöchl, *J. Phys. Chem.* **97** 8617 (1993).
- [24] G. Bester and M. Fähnle, *J. Phys: Cond. Matt.* **13** 11541 and 11551 (2001).
- [25] L. M. Sandratskii and J. Kübler, *Phys. Rev. Lett.* **75** 946 (1995).

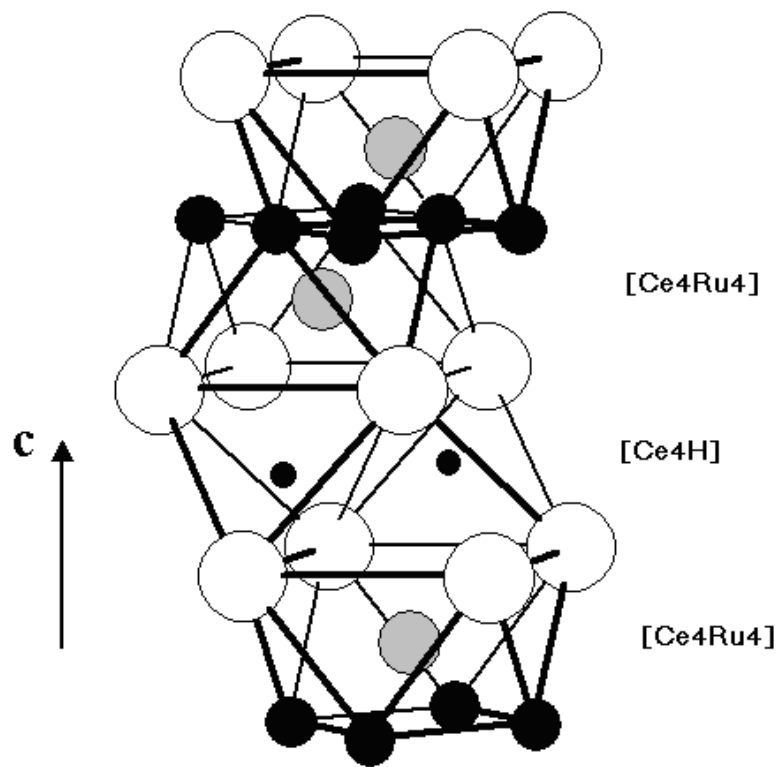
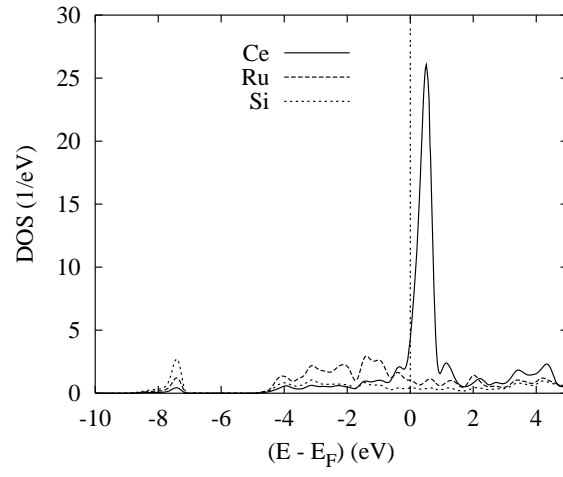
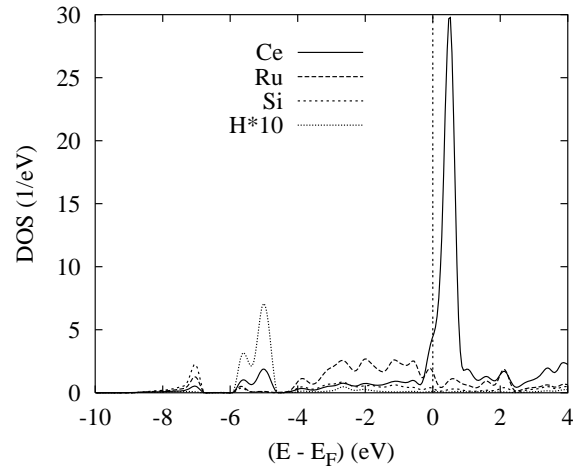


FIG. 1: Sketch of the crystal structure of CeRuSiH. Ce, Ru, Si and H-atoms are represented by white large, black medium, grey medium and black small circles, respectively.

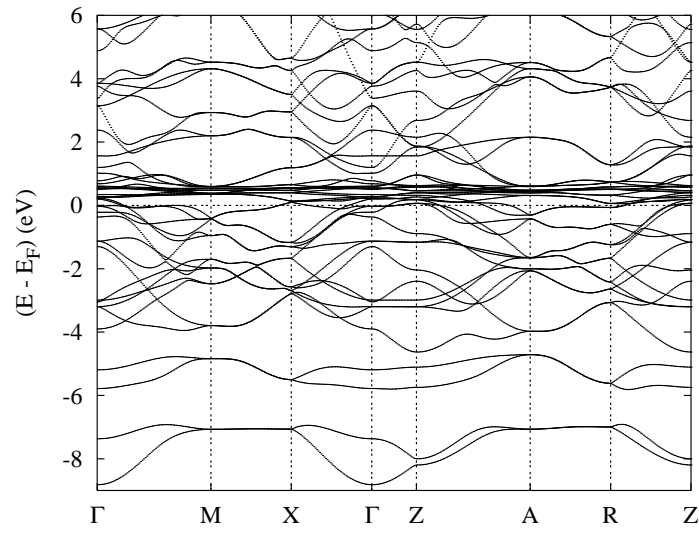


(a) CeRuSi

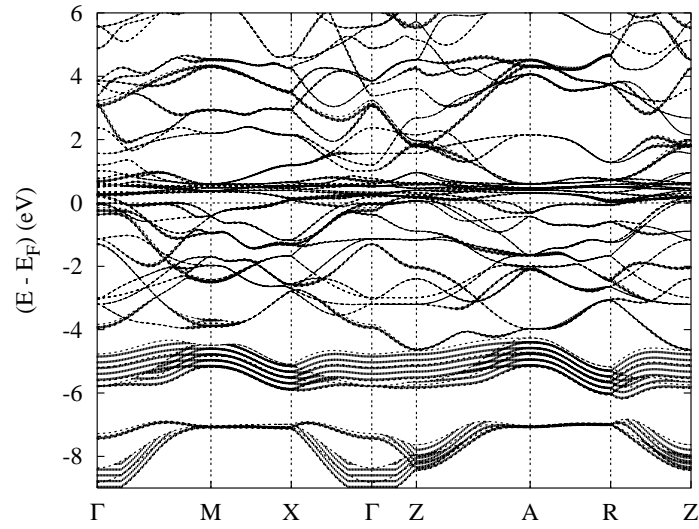


(b) CeRuSiH

FIG. 2: Non magnetic site projected DOS of CeRuSi (a) and CeRuSiH (b).

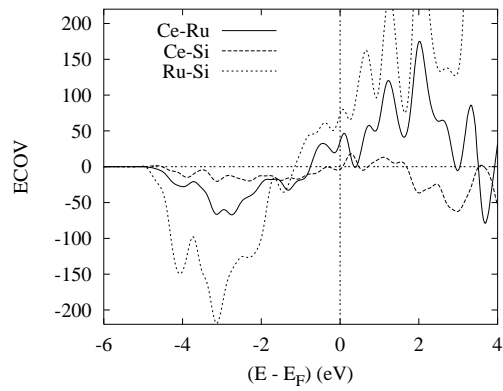


(a) CeRuSiH

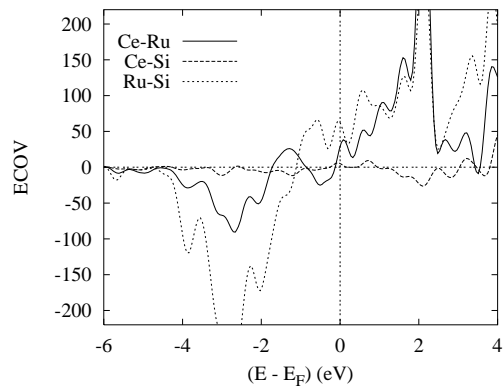


(b) CeRuSiH with hydrogen weighted bands

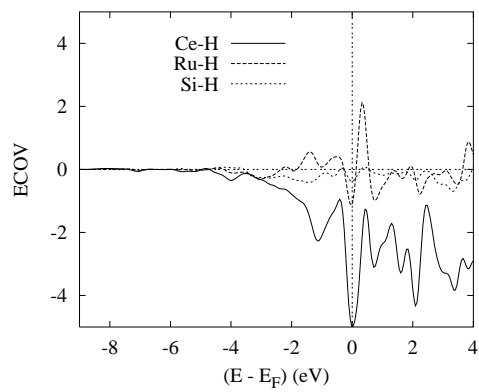
FIG. 3: Band structure of non magnetic CeRuSiH_{1.0} a); H orbital weight are stressed in b).



(a)



(b)



(c)

FIG. 4: Chemical bonding from covalent bond energy criterion (ECOV) for pair interactions within
 a) CeRuSi and its hydride b) and c).

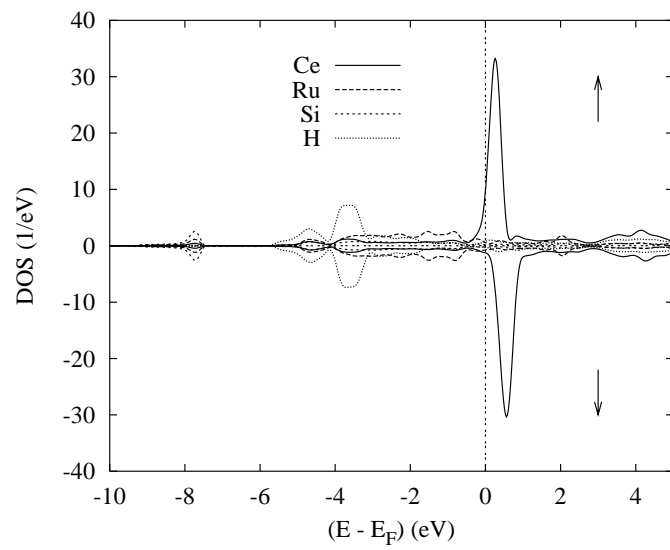


FIG. 5: Site and spin projected DOS of CeRuSiH_{1.0} in the ferromagnetic configuration. Hydrogen PDOS intensity was multiplied by 10 in order to explicit their position.